Clinical Immunology 207 (2019) 24–35

Contents lists available at ScienceDirect

Clinical Immunology

journal homepage: www.elsevier.com/locate/yclim

# The protective effect of interfering TLR9-IRF5 signaling pathway on the development of CVB3-induced myocarditis

Shu Nie[a,b], Boqi Dong[c], Shuang Gao[a], Yan Zhou[b], Wenting Lu[a], Mingli Fang[a], Shucheng Hua[d], Yongli Yu[c,*], Liying Wang[a,*]

[a] Department of Molecular Biology in College of Basic Medical Sciences and Institute of Pediatrics in First Hospital, Jilin University, Changchun 130021, PR China
[b] Department of Pediatric cardiology, The First Hospital of Jilin University, Changchun 130021, PR China
[c] Department of Immunology, College of Basic Medical Sciences, Jilin University, Changchun, Jilin 130021, PR China
[d] Department of Respiratory Medicine, The First Hospital of Jilin University, Changchun 130021, PR China

ARTICLE INFO

*Keywords:*
Coxsackievirus B3
Myocarditis
Toll-like receptor 9
Interferon regulatory factor 5
Oligodeoxynucleotide

ABSTRACT

Since toll-like receptor 9 (TLR9) or interferon regulatory factor 5 (IRF5) was reported to be associated with the development of myocarditis, we wondered if the TLR9-IRF5 pathway could contribute to the development of coxsackievirus B3 (CVB3)-induced myocarditis. We detected signaling molecules of TLR9-IRF5 pathway in CVB3-infected patients and mice. The results showed that TLR9, IRF5 and its downstream molecules such as tumor necrosis factor-α (TNF-α) and interleukin-6 (IL-6) were significantly increased, and the increase was correlated with the severity of heart injury during CVB3 infection. In addition, we demonstrated that an AAAG ODN with IRF5 interfering activities significantly decreased the levels of the TLR9-IRF5 pathway molecules in hearts, spleens as well as white blood cells, and alleviated the myocarditis in CVB3-infected mice. The data suggest that interfering TLR9-IRF5 pathway could be an approach to treat CVB3-induced myocarditis.

## 1. Introduction

Viral myocarditis (VMC), caused by viruses, is inflammation of the heart muscle [1]. Coxsackievirus B3 (CVB3), a type of enteroviruses, is the most common pathogen for the VMC, implicated in 20–40% of VMC patients [2]. Being treated with ribavirin, interferon-beta, immunoglobulins and corticosteroids, CVB3-induced myocarditis remains one of the most challenging clinical problems in cardiology, and still accounts for up to 20–30% of dilated cardiomyopathy in the VMC patients, and 2% to 12% human sudden deaths [1,3]. Thus, novel medications are required to be developed for treating the CVB3-induced myocarditis.

In recent years, the innate immune response induced by CVB3 has been realized to be both beneficial and detrimental to hearts. During the infection, the innate immune cells are activated through recognizing pathogen-associated molecular patterns (PAMPs), such as viral RNAs, by a broad panel of pattern recognition receptors (PRRs), including Toll-like receptors (TLRs), such as TLR9 [4]. TLR9 is activated by the endogenous molecules released from the heart cells damaged by CVB3 replication in the development of the CVB3-induced myocarditis [5,6]. The released molecules, such as high-mobility group box 1 (HMGB1) and mitochondrial DNA (mtDNA), act as damage associated molecular patterns (DAMPs) to initiate sterile inflammatory responses, aggregating the heart damage. The DAMPs activate TLR9 and consequently trigger the recruitment of myeloid differentiation primary response gene 88 (MyD88), interleukin-1 associated kinase (IRAK4) and TNF receptor-associated factor 6 (TRAF6). The TRAF6 in turn activates transforming growth factor activated kinase-1 (TAK1), and subsequently mitogen-activate protein kinase (MAPK) and the IκB kinase (IKK) complex, to activate nuclear factor kappa B (NF-κB). The NF-κB induces the production of inflammatory cytokines, such as tumor necrosis factor-α (TNF-α) and interleukin-6 (IL-6) [7]. The TLR9/MyD88/NF-κB/TNF-α axis, if overly activated, could aggravate CVB3-induced myocarditis, exemplified by the evidences that the VMC mice with deficiency of TLR9 or MyD88 displayed improved left ventricular (LV) function and reduced cardiac inflammation [5,8], and that blocking NF-κB lessens cardiac injury in CVB3-infected mice [9].

In addition to NF-κB, interferon regulatory factor 5 (IRF5) is another downstream transcription factor in TLR9/MyD88 signaling pathways [10]. TLR9 activation induces the formation of MyD88-IRF5-TRAF6 complexes, which in turn activates IRF5 [11]. The activated IRF5 moves from cytoplasm into the nucleus where it binds cis-regulatory elements

* Corresponding authors at: Department of Molecular Biology in College of Basic Medical Sciences or Department of Immunology, College of Basic Medical Sciences, Jilin University, 126 N Xinmin Street, Changchun, Jilin 130021, PR China.
*E-mail addresses:* ylyu@mail.jlu.edu.cn (Y. Yu), wlying@jlu.edu.cn (L. Wang).

https://doi.org/10.1016/j.clim.2019.07.002
Received 1 February 2019; Received in revised form 28 June 2019; Accepted 3 July 2019
Available online 04 July 2019
1521-6616/ 

to promote the transcription of TNF-α and IL-6 [12]. TNF-α is significantly increased in hearts of the CVB3-infected mice. TLR9 deficient mice infected with CVB3 show significantly lower levels of TNF-α in the heart [5]. The increased levels of IL-6 are associated with prognosis of the VMC patients, and injecting an anti-IL-6 receptor antibody reduces CVB3 replication and improves LV functions in the VMC mice [13]. These evidences suggest that TLR9-IRF5 signaling pathway could be involved in the development of CVB3-induced myocarditis, and that IRF5 could be targeted for the treatment of VMC.

To develop IRF5 inhibitors for treating autoimmune/inflammatory diseases, various efforts have been made. Trichostatin A (TSA) capable of depressing promoter activities of IRF5 and reducing productions of TNF-α and IL-6 was tested as a potential drug for the treatment of childhood onset systemic lupus erythematosus (SLE) [14]. Subcutaneously applied sMiR-146b, a microRNA that drives degradation of IRF5 mRNA, ameliorates colitis in mice [15]. An IRF5 decoy peptide binds to IRF5 and reduces IRF5 translocation to the nucleus, therefore reducing myocardial inflammation and improving LV function in mice with systemic sclerosis (SSc) [16]. Interestingly, in our previous work, an AAAG-rich oligodeoxynucleotide (AAAG ODN) was demonstrated to interfere IRF5 activities [17]. The AAAG ODN was designed based on the sequence of human micro-satellite DNA. Coincidentally, the AAAG ODN (5′-AAAGAAAGAAAGAAAGAAAGAAAG-3′) is consensus to the IRF5 binding motif (G/C)(A)AAA(N)$_{2\text{-}3}$AAA(G/C)(T/C) in the regulatory element of TNF-α and IL-6 genes [11]. The AAAG ODN was demonstrated to rescue mice from bacterial septic peritonitis [18] and attenuate burn-induced systemic inflammatory responses in mice [19]. Moreover, the AAAG ODN was found to lessen acute lung inflammatory injury by reducing TNF-α production in the mice infected by influenza virus [17]. Together with these findings, we could propose that the AAAG ODN may alleviate the CVB3-induced myocarditis through interfering TLR9-IRF5 signaling pathway.

To confirm this, in this study, we assessed the levels of TLR9, IRF5, TNF-α and IL-6 in pericardial fluids of the VMC patients, and tested whether the AAAG ODN could lessen myocarditis by interfering TLR9-IRF5 signaling pathway in the mice. The data obtained suggest that the activation of TLR9-IRF5 pathway is involved in the pathogenesis of CVB3-induced myocarditis and inhibiting the pathway could be a novel treatment for VMC.

## 2. Materials and methods

### 2.1. Patients and pericardial fluid collection

From January 2016 - July 2018, in the First hospital of Jilin University, Changchun, P.R.China, 7 patients with viral myocarditis (VMC) and 7 patients with congenital heart disease (CHD) were investigated. The VMC patients were clinically diagnosed with coxsackievirus B-IgM positive blood plus at least two of the four following criteria established by the Chinese Heart Association in 1999 [20,21]: Cardiac insufficiency, cardiogenic shock or cardio-cerebral syndrome; cardiac enlargement; abnormal electrocardiogram lasted 4 days longer; elevated levels of creatinine kinase myocardial band (CK-MB), cardiac troponin T (cTnT) or cardiac troponin I (cTnI). The CHD patients, used as a control, include 2 patients with atrial septal defect, 3 patients with ventricular septal defect and 2 patients with tetralogy of fallot. The clinical data of the 14 patients were shown in Table 1. The cardiac size and cardiac function in the VMC and CHD patients were statistically analyzed by student's *t*-test and shown no significant differences ($p < 0.05$). Written consents were obtained from all of the participants or family members and the protocol for collecting clinical samples was approved by Institutional Review Board, the First hospital, Jilin University.

The pericardial fluids of the VMC patients were collected by aspirating under echocardiographic guidance, while the fluids of the CHD patients were extracted using 10 ml syringe during open-heart surgery.

**Table 1**
The clinical data of patients (mean ± SEM).

| | VMC patients | CHD patients |
|---|---|---|
| Participants (n) | 7 | 7 |
| Age (years) | 5.6 ± 2.9 | 4.7 ± 1.6 |
| Gender | | |
| Male (n) | 5 / 7 | 4 / 7 |
| Female (n) | 2 / 7 | 3 / 7 |
| Course of VMC (days) | 5.7 ± 6.3 | 0 |
| Clinical Sign | | |
| Cardiac insufficiency (n) | 1 / 7 | 0 / 7 |
| Cardiogenic shock (n) | 1 / 7 | 0 / 7 |
| Cardio-cerebral syndrome (n) | 0 | 0 |
| Heart function (NYHA) | 3.1 ± 0.9 | 3.1 ± 0.9 |
| LAD (mm) | 12.7 ± 2.2 | 14.3 ± 1.1 |
| LVEDs (mm) | 34.6 ± 9.8 | 30.8 ± 7.8 |
| LVEDd (mm) | 53.1 ± 10.8 | 50.6 ± 9.3 |
| EF (%) | 49 ± 9.8 | 52.9 ± 3.2 |
| CTR | 0.55 ± 0.08 | 0.49 ± 0.04 |
| Arrhythmia | | |
| Sinus tachycardia (n) | 2 / 7 | 1 / 7 |
| Supraventricular tachycardia (n) | 1 / 7 | 0 / 7 |
| Atrioventricular block (n) | 2 / 7 | 0 / 7 |
| Blood test | | |
| CVB3-IgM + (n) | 7 / 7 | 0 / 7 |
| CK-MB (U / L) (normal range 0–25 U / L) | 76.9 ± 8.9 | 23.4 ± 4.8 |
| cTnI (ng / ml) (normal range 0–0.034 ng / ml) | 0.12 ± 0.089 | 0.011 ± 0.005 |
| CRP (mg / ml) (normal range 0–3 mg / ml) | 2.9 ± 1.2 | 1.9 ± 0.7 |

Note: VMC, viral myocarditis; CHD, congenital heart disease; NYHA, New York Heart Association; LAD, Left Atrial Diameter; LVEDs, Left Ventricular End-Systolic Diameter; LVEDd, Left Ventricular End-Diastolic Diameter; EF, Ejection Fraction; CTR, Cardiothoracic Ratio; CK-MB, MB isoenzyme of creatine kinase; cTnI, cardiac Troponin I; CRP, C-Reactive protein. The heart functions were assessed with the NYHA Classification, graded as: I, no symptoms with ordinary activity; II, mild limitation of physical activity and symptoms with ordinary physical activity; III, marked limitation of physical activity and symptoms with less than ordinary physical activity; and IV, symptoms with any physical activity or at rest [64].

5 ml pericardial fluids were centrifuged at 300*g* for 10 min to separate cells and supernatants. The cells were used to detect expression of TLR9 and IRF5 by the Western blot. The supernatants were stored at −80 °C for detecting TNF-α and IL-6 by the Cytometric Bead Array.

### 2.2. Oligodeoxynucleotides

Nuclease-resistant phosphorothioate-modified ODNs, including an AAAG ODN (5′-AAAGAAAGAAAGAAAGAAAGAAAG-3′) and a non-specific ODN (5′-CCTCCTCCTCCTCCTCCTCCTCCT-3′), were synthesized in Takara Biotechnology Company (Dalian, China) and diluted in PBS buffer without detectable endotoxin (Limulus amebocytelysate assay, Associates of Cape Cod, Inc.). The non-specific ODN was designed by replacing AAAG motifs in the AAAG ODN with CCT, and used as a control ODN in the mouse experiments.

### 2.3. Virus

The Coxsackievirus B3 (CVB3) obtained from Department of Immunology, Jilin University, Changchun, P.R.China was multiplied in Hela cell line cells, harvested 48 h later by freezing and thawing the infected cells for three times, and stored at −70 °C. Hela cells, from American Type Culture Collection (ATCC), were maintained in Iscove's modified Dulbecco's medium (IMDM) supplemented with 10% heat-inactivated fetal bovine serum (GIBCO). Viral titers were determined by cytopathic effect on Hela cells and expressed as 50% tissue culture infective dose (TCID50) per milliliter.

### 2.4. Mice

Six-week-old specific pathogen-free male BALB/c mice (18 ± 2 g), obtained from the Experimental Animal Center, Jilin University (Changchun, P.R.China), were used for establishing CVB3-induced myocarditis model. The mice were maintained at 22 ± 2 °C with a 12 h light / dark cycle, and had free access to food and water for experiments in accordance with the National Institute of Health Guide for the Care and Use of Laboratory Animals.

### 2.5. Animal experiment

The mouse model of CVB3-infected myocarditis was established by intraperitoneally (i.p.) administration with $10^4$ TCID50 CVB3 in 0.1 ml IMDM. On day 0, 1, 4, 7, 10 and 14 post-infection, six of the mice were randomly sacrificed and their hearts were isolated. The left ventricles were kept in the solution of 10% formaldehyde for pathological analysis and the rest parts of the hearts were used for isolating total RNA.

To study the effect of AAAG ODN on CVB3-induced acute myocarditis, we took four different times to inject i.p. 25 μg AAAG ODN into each mouse, including 1 day prior infection (day −1), stimulate with infection (day 0), day 1 and day 4 post-infection. The mice sham-inoculated with sterile PBS on day 0 were used as normal. After infection, the mice were weighted daily, and valued their clinical manifestations by scores based on the occurrence of the symptoms including lethargy, piloerection, tremors, periorbital exudates, respiratory distress and diarrhea [22]. On day 7 post-infection, all of the mice were bled and sacrificed, then their hearts were isolated. The right ventricle was used for pathological analysis, the left ventricle was used for measuring the necrosis area, the right atrium was homogenized for viral load detection, and the rest part was for isolating total RNA. Meanwhile, the spleens and blood were isolated for detecting TLR9, IRF5, TNF-α, IL-6 expression. Besides, to confirm the effect of the AAAG ODN treatment on day 4 post-infection, we infected another 18 mice. On day 4 post-infection, the mice (6 in each group) were i.p. treated with PBS, control ODN or AAAG ODN (25 μg per mouse), respectively. On day 14, all of the mice were bled and then sacrificed. Their hearts were isolated and divided into three parts, the right atrium, the right ventricle and the rest part. The right atrium was homogenized in 1 ml DMEM containing 2% fetal calf serum, then the supernatants were subjected by the centrifugation at 2000*g* for 10 min at 4 °C for detecting the TNF-α and IL-6 expression, and CVB3 titers, the right ventricles were used for isolating total protein, and the rest parts were used for isolating total RNA. Meanwhile, the spleens and blood were also isolated for detecting TLR9, IRF5, TNF-α, IL-6 expression.

### 2.6. Examination of myocardial necrosis

The myocardial necrosis was represented by the ratio of myocardial necrosis. To generate the ratio, the left ventricles were frozen at −20 °C for 3 h, and then cut perpendicularly to the septum from the apex to the mitral valve into 3 mm slices. The slices were incubated in 1% TTC (2, 3, 5-triphenyltetrazolium chloride from Sigma Chemical, St. Louis, MO) in 0.1 M Tris buffer (pH 7.8) at 37 °C for 15 min, and grossly observed for the necrotic areas. The necrotic areas were unstained, in contrast to the red strained areas presenting nonischemic and viable ischemic areas. The slice was photographed and analyzed with Image 1.38 (NIH, Bethesda, MD) to obtain the myocardial necrosis size and the left ventricle size. The percentage of myocardial necrosis size / left ventricle size was used as the ratio of myocardial necrosis, which indicates the extent of the myocardial necrosis.

### 2.7. Pathological examination of hearts

The heart lesions caused by CVB3-induced myocarditis were represented by the pathological scores. To score the lesions, the ventricles were fixed in 10% neutral formalin, embedded in paraffin, cut into 5 μm-thick sections, stained with hematoxylin and eosin (H&E), and examined by two independent observers. The severity of the heart lesions were graded using a five-point system from 0 to 4 [23]. A '0' score indicates no or questionable infiltration of inflammatory cells. A '1' score indicates very limited focal distribution of myocardial lesions. A score of '2'describes multiple lesions, and '3' describes multiple and regular lesions with some confluence and extensive necrosis. A score of '4' describes the presence of coalescent and pervasive lesions spreading throughout most of the observed tissue.

### 2.8. Quantitative reverse transcription-polymerase chain reaction

Quantitative reverse transcription-polymerase chain reaction (qRT-PCR) was conducted using SYBR Green and Light Cycler 480 system (Roche, Shanghai, China). For RNA preparation, the heart and spleen tissue samples were homogenized, and total RNA was extracted using RNeasy Mini kit (Qiagen, Valencia, CA, USA), reverse transcribed into cDNA using Taqman reverse transcription reagents (Applied Biosystems, Foster city, USA) with random hexamer primer, according to the manufacturer's instructions. The two-temperature cycle of 95 °C for 15 s and 60 °C for 1 min (repeated for 40 cycles) was used. Relative quantities of transcripts were calculated using the $2^{-\Delta\Delta Ct}$ method with GAPDH as a reference. The primers used for qRT-PCR were synthesized by Sangon Biotech (Shanghai, China) and listed as follows (forward and reverse primers, respectively): TLR9: 5′-ACCCTGGAAGAGCTAAAC CTG-3′ and 5′-CAGTTGCCGTCCATGAATAGG-3′; IRF5: 5′-AGCGGGAA GTCAAGACGAAGCTCT-3′ and 5′-CTGAGAACATCTCCAGCAGCA-3′; TNF-α: 5′-GGCTCCAGGCGGTGCTTGTT-3′ and 5′-GGCTTGTCACTCGG GGTTCG-3′; IL-6: 5′-GGATACCACTCCCAACAGACC-3′ and 5′-TCCAGT TTGGTAGCATCATCA-3′; GAPDH: 5′-TGCTGAGTATGTCGTGGA-3′ and 5′-TTCAGCTCTGGGATGACCT-3′.

### 2.9. Western blot

The pericardial fluid cells of VMC patients and the heart tissues of VMC mice were lysed in ice-cold RIPA buffer (150 mM NaCl, 50 mM Tris, pH 7.4, 1% NP-40, 0.5% sodium deoxycholate, 0.1% SDS and PMSF) for protein preparation, respectively. The protein concentration was measured by the BCA method. Western blot analyses were performed using primary antibodies raised against IRF5 (1:500, Abcam), TLR9 (1:1000, Abcam), TNF-α (1:1000, Abcam), IL-6 (1:1000, Abcam) and incubated with 5% milk overnight at room temperature. Chemiluminescence detection was performed with ECL Plus (Amersham Biosciences Hyperfilm, GE Healthcare), detected with the use of X-ray films, and analyzed by densitometric analysis program (Image Gauge V3.12; Fuji Photo Film, Tokyo, Japan). The house keeping gene GAPDH was used as a loading control.

### 2.10. Flow cytometry

The whole blood was harvested from the mice on day 7 and day 14 post-CVB3 infection using the tubes containing 3.8% sodium citrate (1/9 *v*/v). The tubes were centrifuged (2000 *g* at 4 °C) for 5 min. The cell pellet was re-suspended using ACK buffer (1/9 v/v) ($NH_4Cl$ 8024 mg / l, $KHCO_3$ 1001 mg / l, $Na_2EDTA$ 3.7 mg / l, pH 7.2–7.4) for 7–10 min to lyse red blood cells, followed by washing and centrifugating twice. The obtained white blood cells (WBCs) were diluted 1:1 with RMIP1640 medium, then added into a 12-well plate and incubated with monensin (eBioscience) for 2 h in 5% $CO_2$ at 37 °C. Afterwards, the cells were collected, fixed with 4% paraformaldehyde, and permeabilized with 0.1% saponin, followed by staining with APC rat anti-mouse TLR9, FITC rat anti-mouse IRF5, PE-Cy7 rat anti-mouse TNF-α, APC rat anti-mouse IL-6. All stained cells were analyzed by Accuri C6 (BD) and FACSCanto (BD) flow cytometers. Live cells were carefully gated by forward and side scattering. Data were analyzed with FlowJo software (FlowJo

7.6.1, LLC, Ashland, Oregon).

### 2.11. Cytometric bead array

The concentrations of TNF-α and IL-6 in pericardial fluids of the patients and in heart homogenates of the mice were determined by Cytometric Bead Array (CBA), according to the manufacturer's protocol (BD Biosciences) with minor modification. Supernatants of individual pericardial fluids or murine heart homogenates (50 μl) were subjected in duplicate using the CBA kit on a FACS Calibur flow cytometry. The concentrations were quantified using the CellQuestPro and CBA software (Becton Dickinson).

### 2.12. Virus titers

The hearts were removed from the VMC mice and perfused with 10 ml of PBS. The right atrium of the heart was homogenized in 1 ml DMEM containing 2% fetal calf serum. The cellular debris was removed by centrifugation at 2000 *g* for 10 min at 4 °C. Following 10-fold serial dilutions in DMEM, 200 μl of supernatants was added in triplicate to a confluent monolayer of Hela cells on a 12-well plate and incubated at 37 °C and 5% $CO_2$. The CVB3 titers were expressed as TCID50 assays, calculated by the method of Reed & Muench Reed [24]. Results were read on day 4–7 after infection.

### 2.13. Statistical analysis

Statistical analyses were conducted using SPSS 19.0 software. A Student's test was used for two-group comparisons, and one-way analysis of variance (ANOVA) for three or more-group comparisons. $P < 0.05$ was considered to be statistically significant.

## 3. Results

### 3.1. The expression of TLR9, IRF5, TNF-α and IL-6 in patients with CVB3-induced myocarditis

To explore whether the TLR9-IRF5 pathway is activated during the development of CVB3-induced myocarditis, we collected pericardial fluids from the VMC patients with CVB3 infection and the CHD patients without CVB3 infection, and tested their levels of TLR9, IRF5 by Western blot. As shown in Fig. 1 A, the levels of TLR9 and IRF5 protein were increased by 22% and 14%, respectively, in the pericardial fluids from the VMC patients as compared with those from the CHD patients, indicating that the CVB3 infection could induce the expression of TLR9 and IRF5 in hearts. Since the TLR9-IRF5 signaling drives the production of TNF-α and IL-6 from inflammatory cells [11], we next tested the levels of TNF-α and IL-6 in the pericardial fluids by Cytometric bead array (CBA). The results showed that levels of TNF-α and IL-6 were obviously elevated in the pericardial fluids of VMC patients, compared to those in CHD patients ($p < .05$) (Fig. 1 B). Together, these observations support that the TLR9-IRF5 pathway could be activated in hearts of the VMC patients with CVB3 infection.

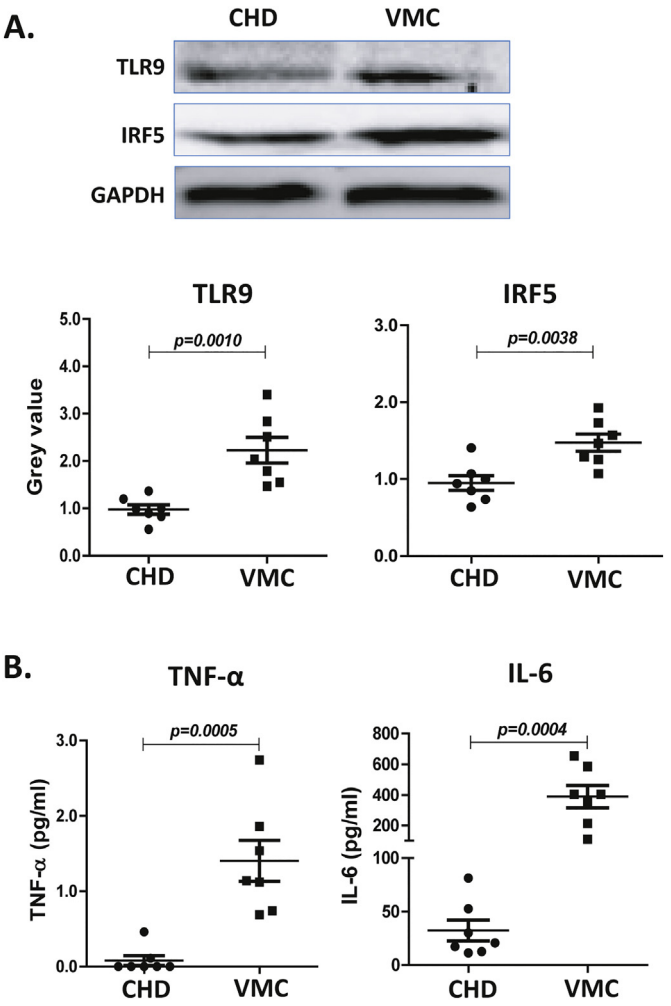


**Fig. 1.** TLR9, IRF5, TNF-α and IL-6 levels in pericardial fluids of VMC patients. The cells and supernatants in pericardial fluids were collected from 7 VMC patients and 7 CHD patients without CVB3 infection for detecting the expression of TLR9, IRF5, TNF-α and IL-6. (A) Western blot detection of the TLR9 and IRF5 in the cells. (B) Cytometric bead array (CBA) detection of the TNF-α and IL-6 in the supernatants. Each symbol represents one patient. Horizontal lines represent means.

### 3.2. The effect of TLR9-IRF5 signaling on cardiac injury of VMC mice

Upon the findings that activation of the TLR9-IRF5 pathway is related to the VMC development in human, we infected mice with $10^4$ TCID50 CVB3 intraperitoneally on day 0 to induce myocarditis. On day 1, 4, 7, 10, and 14 post-infection, the mice were randomly sacrificed and their hearts were separated into the left ventricles and the rest parts. The left ventricle was used to observe the pathological lesions, and the rest part was tested for mRNA levels of signaling molecules in TLR9-IRF5 pathway, including TLR9, IRF5, TNF-α and IL-6. Pathological observations showed minimally infiltrated lymphocytes in the hearts on day 1 post-CVB3 infection. The infiltration became apparent on day 4, peaked on day 7, and then gradually reduced until day 14. Notably, the hearts displayed extensive lesions with massive necrosis of the myocytes on day 7 post-infection. The lesions were quantitatively evaluated with the pathological scores, which increased from day 4 ($p = .013$) and peaked on day 7 post-infection ($p = .005$) (Fig. 2 A). The mRNA detection showed that the CVB3 induced obviously elevated expression of TLR9, IRF5, and IL-6 mRNAs on day 4 post-infection and peak expression of IRF5 mRNA on day 7 ($p = .012$). Interestingly, CVB3 induced the steadily increased TLR9 expression and decreased IL-6 expression up to the day 14, and induced the significantly increased expression of TNF-α mRNA on day 7 post-infection ($p = .046$) (Fig. 2 B and C). These results indicated that vigorous activation of the TLR9-IRF5 signaling pathway could be involved in the cardiac injury induced by CVB3 infection.

### 3.3. The roles of AAAG ODN on CVB3-induced myocarditis in mice

Since the AAAG ODN was demonstrated to alleviate acute lung injury caused by influenza virus infection [17], we were curious to find whether the AAAG ODN could also alleviate the CVB3-induced inflammatory damage in hearts. To start with, the CVB3-infected mice (3 / group) were treated with AAAG ODN once on day −1, 0, 1, or 4 prior

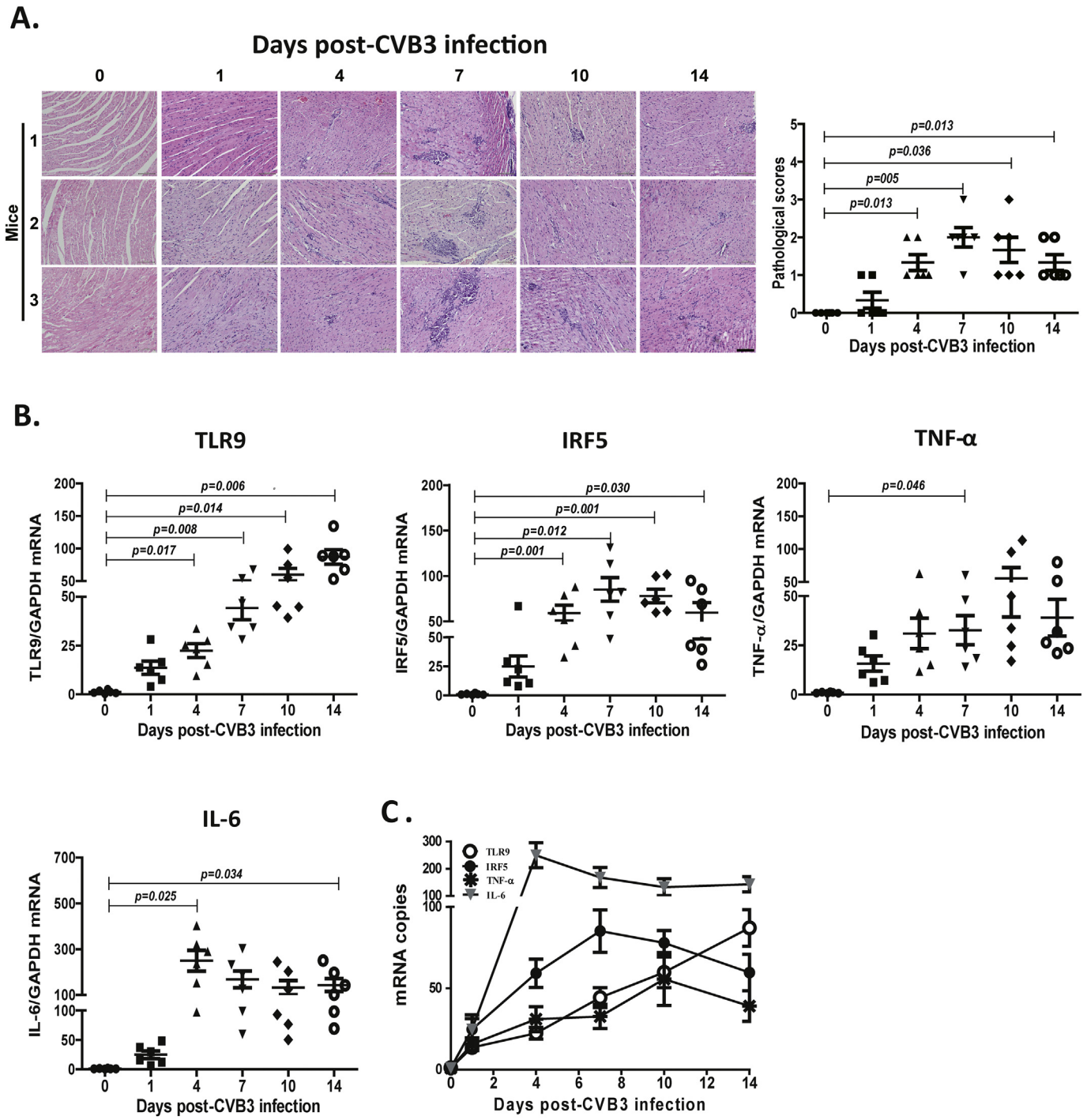


**Fig. 2.** Expressions of TLR9-IRF5 pathway molecules in myocardial tissues from.
CVB3-infected mice. The mice were infected with CVB3 on day 0 and sacrificed on day 1, 4, 7, 10, 14 post-CVB3 infection for isolating their hearts. (A) The pathological changes (× 200) and scores of H&E stained heart tissues. Scale bar, 200 μm. (B) qRT-PCR analysis on the kinetically expressed mRNAs of TLR9, IRF5, TNF-α and IL-6. Each symbol represents one mouse. Horizontal lines represent means. (C) The comparison of the kinetic expression of the mRNAs. Each symbol represents the mean and standard deviation of data from the six mice. Data of one representative experiment from the three are shown.

or post-infection, respectively, at a dose of 25 μg / mouse as used in our previous work [25,26], and were weighted and observed daily. On day 7 post-infection, the mice were sacrificed and their hearts were pathologically analyzed. It was found that the AAAG ODN treatment once on day 4 post-infection obviously improved the general status, and dramatically lessened the heart damage of the VMC mice, while the AAAG ODN treatment on −1, 0 and 1 day failed to. To confirm the efficacy and to find whether the efficacy was sequence dependent, we conducted a set of mouse experiments, in which 6 mice were used in each group and a control ODN was included to verify the sequence specificity of the AAAG ODN, to detect the roles of AAAG ODN on CVB3-induced myocarditis and the influence of AAAG ODN on TLR9-IRF5 pathway in the heart, spleen, white blood cells as well as on the cardiac viral load. On day 0, the mice were infected with CVB3, treated with AAAG ODN (i.p. 25 μg / mouse) on day −1, 0, 1, or 4, or treated with control ODN on day 4, respectively, afterwards, were weighted and observed daily. Compared with that of the PBS group, the body weight of the CVB3-infected mice treated with AAAG ODN on day 4

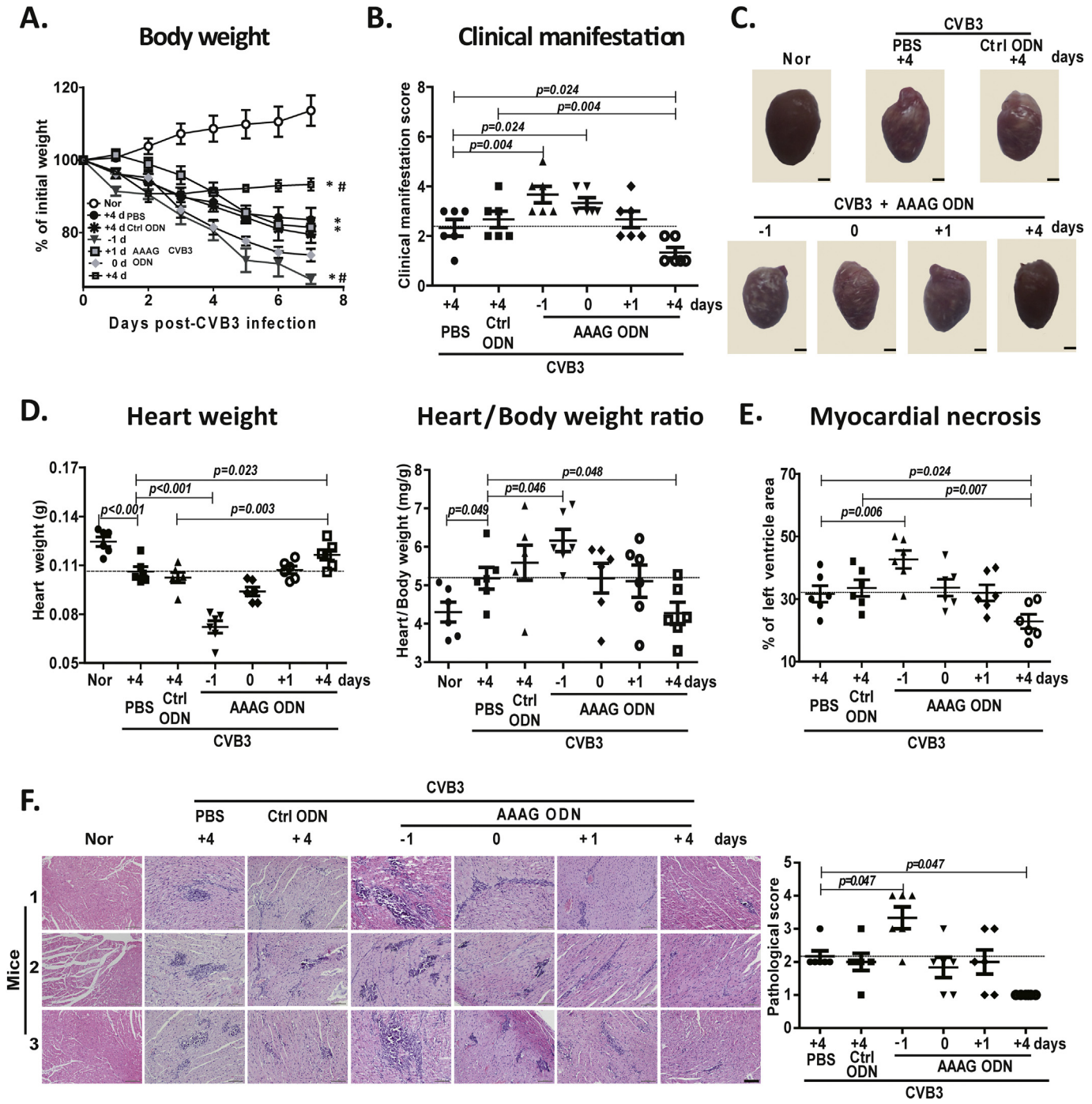


**Fig. 3.** Influence of AAAG ODN on CVB3-induced myocarditis in mice. The mice were infected with CVB3 on day 0 and treated with AAAG ODN or Ctrl ODN before or after the infection, respectively, and observed / weighted daily. On day 7 post-infection, the mice were sacrificed and their hearts were isolated for surface observation, weighting, necrosis area measurement and pathological examination. (A) The body weight of the mice ($n$ = 6 mice / group). $_{*}p < .05$ vs that in normal mice; # $p < .05$ vs that in the mice treated with PBS. (B) The clinical manifestation score of the mice on day 7 post-infection. (C) The surface observation of the hearts. Scale bar, 2 mm. (D) The heart weight and heart / body weight ratio of the mice. (E) The percentage of necrosis area to the left ventricle area of the hearts. (F) The pathological changes (× 200) and scores of H&E stained heart tissues of the mice. Scale bar, 200 μm. Each symbol represents one mouse. Horizontal lines represent means. Data from one representative experiment of the three are shown. Nor, normal; Ctrl ODN, control ODN.

post-infection declined slightly, whereas the body weight of the mice treated with AAAG ODN on day −1 underwent a dramatic and continuous loss, up to 35% on day 7 post-infection (Fig. 3 A). With the reference that > 70% BALB/c mice died post-HSV infection when their body weights lost up to 20% [27], we ended the experiments on the day 7 post-CVB3 infection. Interestingly, we found that the AAAG ODN treatment on day 4 significantly improved the clinical manifestations of the CVB3-infected mice ($p$ = .024), while the AAAG ODN treatment on day −1 ($p$ = .004) and day 0 ($p$ = .024) worsened the clinical manifestations, and on day 1 failed to improve the clinical manifestations (Fig. 3 B).

To determine whether the improvement was relevant to the alleviation of the CVB3-induced inflammatory responses in hearts, we further examined the pathological changes of the hearts on day 7 post-infection. As shown in Fig. 3 C, on the surface of the hearts, CVB3 infection induced the obvious tan-yellow marbling, an indicator of severe

inflammation, eosinophilic degeneration, calcification, or fibrosis [28]. The AAAG ODN treatment on day 4 significantly reduced the extent of the tan-yellow marbling. In contrast, the AAAG ODN treatment on day −1 aggravated the marbling. Besides, the heart weight and the heart / body weight ratio were used to evaluate the cardiac edema and necrosis [29]. As shown in Fig. 3 D, the AAAG ODN treatment on day 4 increased the heart weights ($p = .023$) and reduced the heart / body weight ratio ($p = .048$), while the treatment on day −1 decreased the heart weight ($p < 0.001$) and increased the ratio ($p = .046$). Also, the AAAG ODN treatment on day 4 significantly deceased the cardiac necrosis areas of the mice ($p = .024$), while the treatment on day −1 ($p = .006$) increased the areas (Fig. 3 E). Histological analysis revealed that the AAAG ODN treatment on day 4 markedly reduced the foci of inflammation (clusters of cells that stain blue) and cell necrosis (areas of clearance) in hearts, led to decreased pathological scores ($p = .047$). In contrast, the treatment on day −1 induced the severe myocarditis manifested by tissue damage and massive inflammatory cell infiltration, with the increased pathological scores ($p = .047$) (Fig. 3 F). The AAAG ODN treatment on day 0 and on day 1 failed to display therapeutic effect on the hearts of the CVB3-infected mice, compared with the PBS treatment. Suggestively, the day 4 post-infection should be an appropriate time point to use the AAAG ODN for treating the CVB3-induced myocarditis.

### 3.4. The influence of AAAG ODN on TLR9-IRF5 pathway in heart of mice with CVB3-induced myocarditis

As above, CVB3 infection significantly elevated the levels of TLR9, IRF5 and their downstream cytokines (TNF-α and IL-6) in hearts, and the AAAG ODN treatment on day 4 was therapeutic on the CVB3-induced myocarditis, we tried to find whether the AAAG ODN could influence the expressions of TLR9-IRF5 pathway molecules, including TLR9, IRF5, TNF-α and IL-6. The mice were infected with CVB3 on day 0, treated with AAAG ODN (i.p. 25 μg / mouse) on day −1, 0, 1, or 4, or treated with control ODN on day 4, respectively. On day 7 post-infection, the mice were sacrificed to test the mRNA expressions of TLR9-IRF5 pathway molecules in hearts. As shown in Fig. 4 A, the AAAG ODN treatment on day 4 significantly decreased cardiac mRNA expression of TLR9 ($p = .017$), IRF5 ($p = .044$), TNF-α ($p = .025$) and IL-6 ($p = .040$), respectively. In contrast, the AAAG ODN treatment on day −1 significantly increased cardiac mRNA expressions of TLR9 ($p < 0.001$), IRF5 ($p = .041$), TNF-α ($p = .044$), respectively, and decreased the IL-6 expression ($p = .024$). Whereas the AAAG ODN treatment on day 0 only increased the TLR9 ($p = .007$) expression, and the treatment on day 1 only decreased the IL-6 expression ($p = .037$) (Fig. 4 A). Besides, to confirm the effect of AAAG ODN treatment on day 4 post-infection, we infected the mice (6 in each group) on day 0 and treated (i.p.) mice with AAAG ODN, PBS or control ODN, respectively, on day 4 post-infection. On day 14 post-CVB3 infection, the mice were sacrificed and their hearts were isolated to assess the mRNAs and proteins of TLR9, IRF5, TNF-α and IL-6. Consistently, the AAAG ODN treatment on day 4 post-infection significantly decreased the cardiac mRNA expressions of TLR9 ($p = .004$), IRF5 ($p = .004$), and TNF-α ($p = .001$) (Fig. 4 B) and the protein expressions of TLR9 ($p = .026$), IRF5 ($p = .026$), TNF-α ($p = .016$) detected by western blot (Fig. 5 A), respectively. Interestingly, the cardiac mRNA expression ($p = .001$) and protein expression ($p = .001$) of IL-6 were significantly increased in the mice treated with AAAG ODN on day 4 (Fig. 4 B and 5 A). Alternatively, we also detected the TNF-α and IL-6 in the heart homogenates by the CBA as described in methods and found that the AAAG ODN treatment on day 4 significantly decreased the TNF-α ($p = .029$) and increased the IL-6 ($p = .030$) (Fig. 5 B), respectively. These results suggested that the AAAG ODN treatment on day 4 could alleviate the CVB3-induced myocarditis by suppressing the expression of the TLR9-IRF5 pathway molecules in hearts.

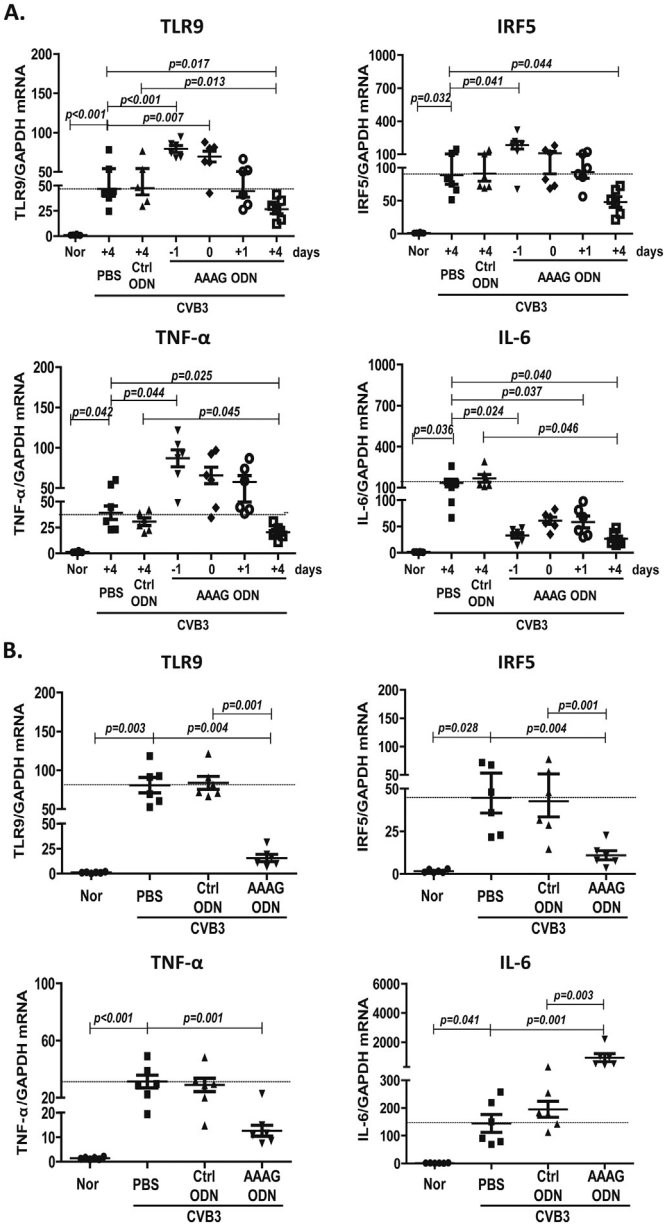


**Fig. 4.** Effect of AAAG ODN on mRNA expression of TLR9-IRF5 pathway molecules in hearts of the mice with CVB3-induced myocarditis. The mice were infected with CVB3 on day 0 and treated with AAAG ODN or Ctrl ODN before or after the infection, respectively. On day 7 or day 14 post-infection, the hearts of the mice were isolated for analyzing the mRNA levels of TLR9, IRF5, TNF-α and IL-6. (A) The mRNA levels on day 7. (B) The mRNA levels on day 14. Each symbol represents one mouse. Horizontal lines represent means. Data from one representative experiment of the three are shown. Nor, normal; Ctrl ODN, control ODN.

### 3.5. The effect of AAAG ODN on expression of TLR9-IRF5 pathway molecules in peripheral immune cells of the mice with CVB3 infection

Next, we explored whether the AAAG ODN could influence the inflammatory responses in hearts by acting on the spleen cells and the white blood cells (WBCs) in periphery. The CVB3-infected mice were treated with AAAG ODN on day −1, 0, 1, or 4, respectively. On day 7 or 14 post-CVB3 infection, we isolated the spleen cells and WBCs, and assessed their activation of the TLR9-IRF5 pathway molecules. The results showed that in the spleen cells, the AAAG ODN treatment on day 4 decreased the mRNA expressions of TLR9 ($p = .049$), IRF5 ($p = .042$) and TNF-α ($p = .049$); the treatment on day −1 increased the

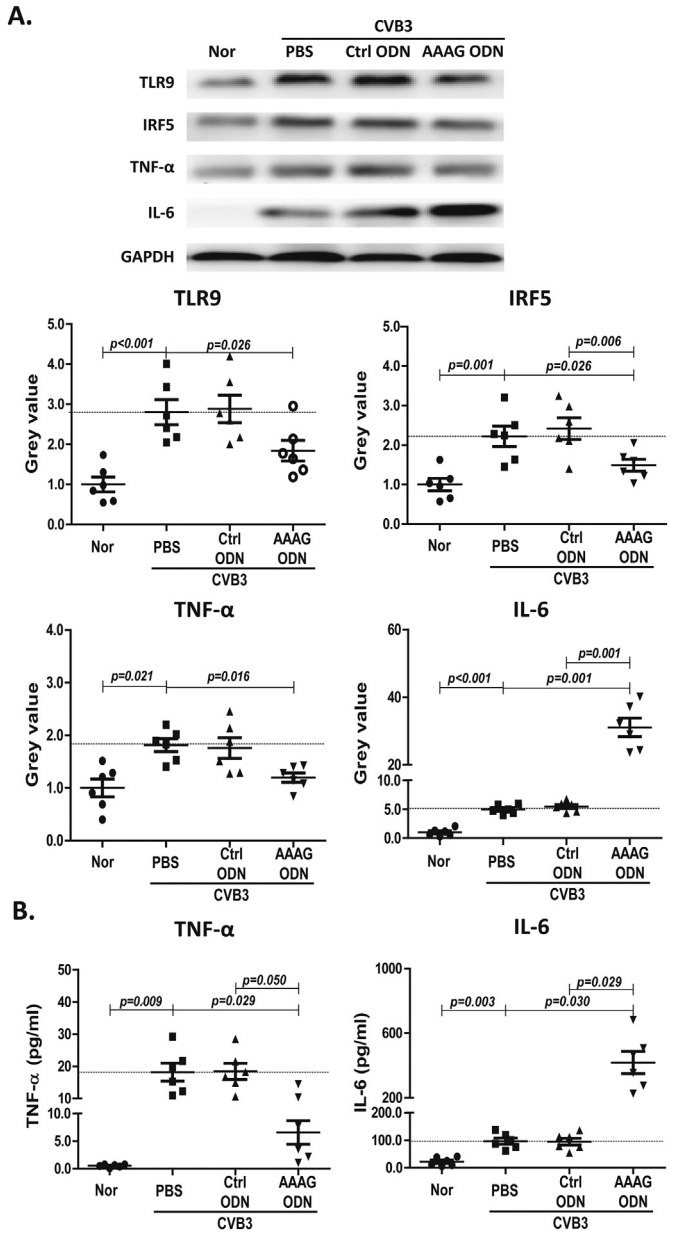


**Fig. 5.** Effect of AAAG ODN on protein levels of TLR9-IRF5 pathway molecules. in hearts of the mice with CVB3-induced myocarditis. The mice were infected with CVB3 on day 0 and treated with AAAG ODN or Ctrl ODN on day 4 for detecting the protein expressions of TLR9, IRF5, TNF-α, IL-6 in their hearts on day 14 post-infection. (A) Western blot detection of the TLR9, IRF5, TNF-α, IL-6 in the heart tissues. (B) Cytometric bead array (CBA) detection of the TNF-α and IL-6 in the heart homogenates. Each symbol represents one mouse. Horizontal lines represent means. Data from one representative experiment of the three are shown. Nor, normal; Ctrl ODN, control ODN.

expressions of TLR9 ($p = .031$), IRF5 ($p = .047$) and TNF-α ($p = .008$) on day 7 (Fig. 6 A); The increases and the decreases couldn't be detected on day 14 (Fig. 6 B). By using flow cytometry, we found that the AAAG ODN treatment on day 4 decreased the expressions of TLR9 ($p < 0.001$), IRF5 ($p = .016$) and TNF-α ($p = .048$) proteins in WBCs of the mice on day 7 (Fig. 6 C), and didn't influence the expressions of the TLR9-IRF5 pathway molecules on day 14 (Fig. 6 D).The results indicate that the AAAD OND treatment on day 4 participates in the myocardial inflammatory responses in the mice by regulating the immune cells in periphery.

### *3.6. The effect of AAAG ODN on the CVB3 load in hearts of the mice with CVB3 infection*

To see if the AAAG ODN could influence the CVB3 load in hearts, the CVB3-infected mice were treated with AAAG ODN on day 4 post-infection and sacrificed on day 7 or 14, respectively, for detecting the CVB3 load in their hearts. The results shows that the cardiac CVB3 titers of the mice treated with the AAAG ODN were within the same range as that of the mice treated with the PBS (Fig. 7), suggesting that the AAAG ODN couldn't induce the inhibition on CVB3.

## 4. Discussion

In this study, we have found that TLR9-IRF5 pathway is activated during the development of CVB3-induced myocarditis, and interfering its activation lessens the detrimental inflammation in hearts. Based on the findings and the data from other labs, we may propose a model (Fig. 8) about how the TLR9-IRF5 pathway is activated during the CVB3 infection and involved in the development of CVB3-induced myocarditis. Although unable to directly sense CVB3 by recognizing the nucleic PAMPs derived from the CVB3 replication, TLR9 does recognize the damage associated molecular patterns (DAMPs) released from the CVB3-damaged cadiomyocytes [5,8,21,30,31]. The DAMPs, such as HMGB1 [32] and mtDNA [31], are sensed by TLR9s expressed in cardiomyocytes, denditic cells, neutrophils and macrophages in hearts [34,35]. The HMGB1 [36] and/or mtDNAs [33] activate TLR9 and trigger the production of pro-inflammatory cytokines [37]. Thus, a positive feedback loop apparently exists. The DAMPs released from the damaged cadiomyocytes during CVB3 infection amplify the inflammatory responses, which in turn damage the cadiomyocytes causing further release of the DAMPs. In the loop, TLR9 could serve as an endogenous sensor of heart damage, and its activation could be causally linked to the development of VMC. The linkage could be evidenced by the findings that TLR9 deficiency improved LV function and decreased cardiac inflammation in the VMC mice [5], and by the observations in this study that the decreased expression of TLR9 in the hearts was associated with improved clinical manifestations and reduced cardiac injury. After being activated, the TLR9 recruits and activates MyD88 which initiates two distinctive signaling pathways using NF-κB and IRF5 as downstream transcription factors, respectively [38]. By far, the activation of the TLR9-NF-κB signaling pathway has been documented as a common cause of the inflammatory injury of hearts after CVB3 infection [9]. In this study, TLR9-IRF5 signaling pathway was revealed pivotal in the development of CVB3-induced myocarditis, possibly other inflammatory diseases. Evidently, IRF5 activation was associated with SLE [14], rheumatoid arthritis [39] and inflammatory bowel disease [40], and the individuals with deficient expression of IRF5 were invulnerable to develop lethal shock induced by a TLR9 agonist [11].

To verify the roles of the TLR9-IRF5 signaling pathway in the development of CVB3-induced myocarditis, we used the AAAG ODN to intervene the IRF5 activity. Structurally, AAAG ODN is consensus with the IRF5 binding site in the regulatory element of genes for TNF-α and IL-6 [11,17,41]. The sequence similarity could render the AAAG ODN to bind IRF5. The binding was demonstrated to hinder the nuclear translocation of IRF5 [18] and to compete with the regulatory element to bind IRF5, and therefore interfering IRF5 to drive the transcription of genes for TNF-α and IL-6 [19]. By doing this, the AAAD ODN could reduce the production of pro-inflammatory cytokines in CVB3-infected patients and mice. The presumption could be strengthened by the presented data that the AAAG ODN, when applied on day 4 post-infection, significantly reduced the production of TNF-α and IL-6 in the hearts, and the production of TNF-α in peripheral immune cells of the mice on day 7 post-CVB3 infection when the AAAG ODN was applied on day 4. Interestingly, as shown in Fig. 4B and Fig. 5B, the mRNA expression and the protein expression of the IL-6 were significantly

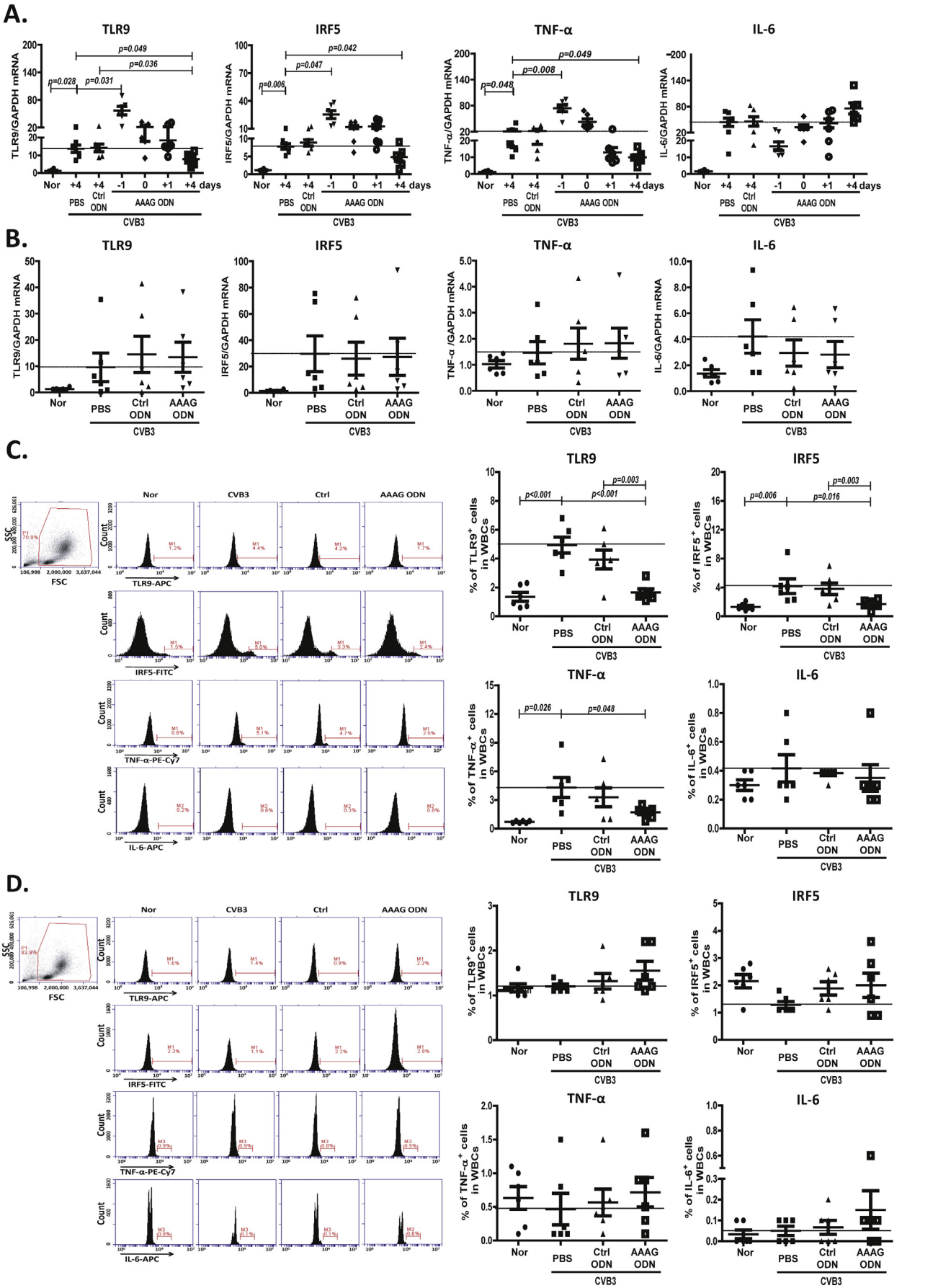


*(caption on next page)*

**Fig. 6.** Effect of AAAG ODN on TLR9-IRF5 pathway molecules in peripheral immune cells of the mice with CVB3 infection. The mice were infected with CVB3 on day 0 and treated with AAAG ODN or Ctrl ODN before or after the infection, respectively. On day7 or day 14 post-infection, the spleens of the mice were isolated for mRNA analysis of the TLR9, IRF5, TNF-α and IL-6 by qRT-PCR, and the white blood cells (WBCs) in peripheral blood of the mice were harvested for protein detection of the TLR9, IRF5, TNF-α and IL-6 by flow cytometry. (A) The mRNA levels in the spleens on day 7. (B) The mRNA levels in the spleens on day 14. (C) The protein levels in the WBCs on day 7. (D) The protein levels in the WBCs on day14. Each symbol represents one mouse. Horizontal lines represent means. Data from one representative experiment of the three are shown. Nor, normal; Ctrl ODN, control ODN.

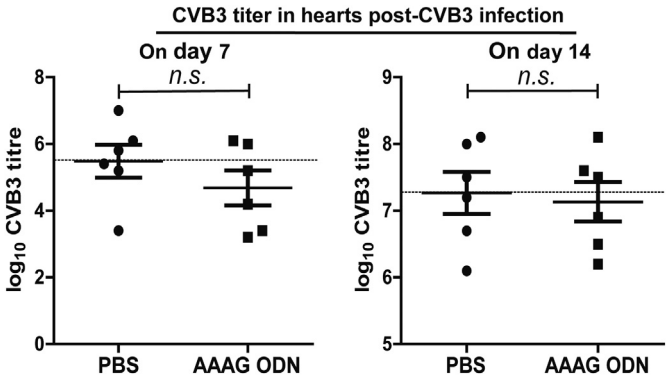


**Fig. 7.** Viral load in hearts of the CVB3-infected mice treated with AAAG ODN. The mice were infected with CVB3 on day 0 and treated with PBS or AAAG ODN on day 4 post-infection for titering the CVB3 in their hearts on day 7 and 14 post-infection. Each symbol represents one mouse. Horizontal lines represent means. Data from one representative experiment of the three are shown. n.s. denotes the insignificance.

increased in the hearts of the mice on day 14 post-CVB3 infection. Obviously, the increase could not be explained by the AAAG ODN mediated interferences of IRF5 to prime the IL-6 gene transcription. However, the increase could be attributed to the heart recovery of the mice treated with AAAG ODN. In the process of heart recovery, a large amount of IL-6 is produced by myocytes in the mice experienced myocarditis-induced cardiac damage [42]. The abundantly produced IL-6 is associated with activation of adenosine monophosphate-activated protein kinase (AMPK) [43,44]. As an energy sensor, AMPK is activated by adenosine monophosphate (AMP) which is dramatically generated during the heart recovery [45], whose activation eventually increases the catabolic metabolism and the IL-6 production [43,44,46]. Importantly, the myocyte-derived IL-6 in turn induces more IL-6 in an autocrine manner [47]. In this setting, the abundantly existed IL-6 exerts cardio-protection by sustaining the vitality of myocytes [48,49], and by reducing the production of TNF-α [50,51], a sufficiently cardiodepressive cytokine in the development of CVB3-induced myocarditis [5]. Taken together, we may propose that suppressing TLR9-IRF5 pathway could be a major underlining mechanism for the AAAG ODN to alleviate CVB3-induced myocarditis. Potentially, as demonstrated in our previous work, the AAAD ODN could be also used for the treatment of other inflammatory diseases, such as bacterial septic peritonitis [18], burn-induced systemic inflammatory response syndrome caused by burning [19], and acute lung inflammatory injury induced by influenza virus [17].

Noticeably, as shown in Fig. 3, CVB3 infection reduced the heart weight on day 7 post-infection, especially in the mice treated with AAAG ODN on day −1. The deteriorated effect of the AAAG ODN could be attributed to the immune restoration which refers to the erratic immune response before / after using immunomodulatory drugs and the resultant immunopathological abnormality in tissues infected by pathogens. The immune restoration may lead to immune restoration diseases (IRD). The IRD could be exemplified by that the patients received antiviral therapy were vulnerable to developing cryptococcal meningitis which was paralleled with reactivation of monocytes and pathological overproduction of cytokines [52]. Presumably, the AAAG ODN treatment on day −1 post-CVB3 infection may condition the mice to launch erratic immune responses to the coming CVB3 infection. As

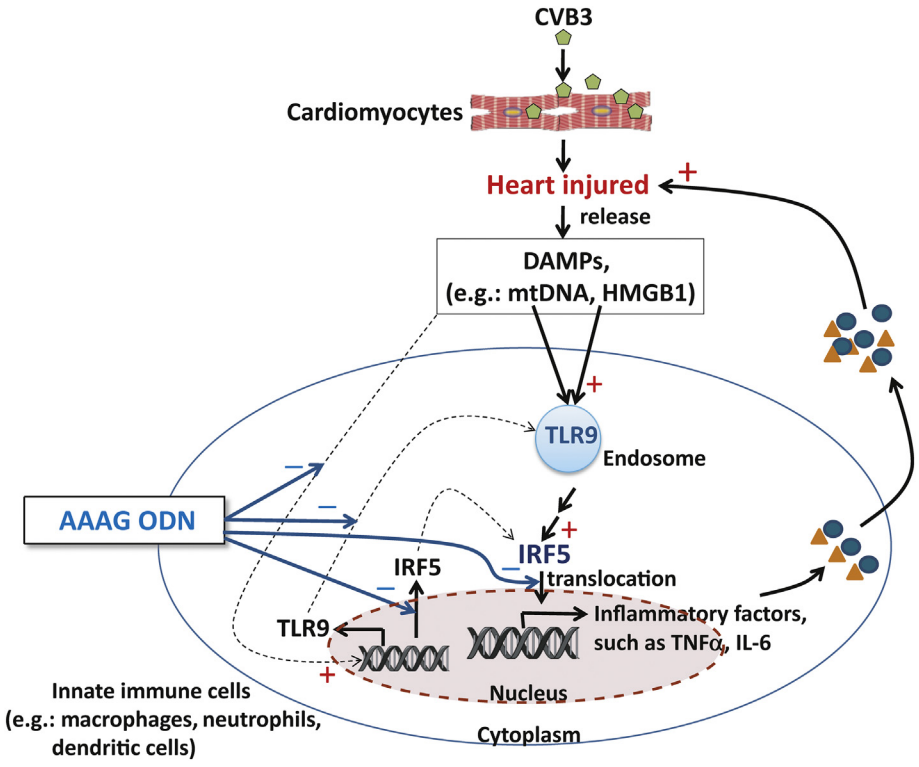


**Fig. 8.** Schematic representation of possible roles of the TLR9-IRF5 signaling pathways in the development of CVB3-induced myocarditis. The damage associated molecular patterns (DAMPs), such as HMGB1 and mtDNA, released from the CVB3-damaged cadiomyocytes could activate the TLR9-IRF5 signaling pathway, leading to excessive production of TNF-α and IL-6. The cytokines could aggravate the cadiomyocyte damage, causing the release of more DAMPs. The AAAG ODN could alleviate the CVB3-induced myocarditis by interfering the TLR9-IRF5 signaling pathway.

shown in this study, the mice received the AAAG ODN prior to the CVB3 infection were detected with significantly higher level of TLR9, IRF5 and TNF-α in the white blood cells, spleens and hearts, reflecting the over-activation of TLR9-IRF5 pathway, that was in parallel with the severity of heart injury. Interestingly, administration of the AAAG ODN on day 4 post-infection could avoid inducing immune restoration. Moreover, the AAAG ODN applied at this time point beneficially suppressed the expression of TLR9-IRF5 pathway molecules and therefore alleviated the CVB3-induced myocarditis. Possibly, the immune restoration induced by the priorly applied AAAG ODN could be used to explain the most significant decrease of heart weight in the CVB3-infected mice. The mice conditioned by AAAG ODN produced higher level of proinflammatory cytokines, such as TNF-α. The TNF-α was reported to evoke catabolic reaction that promotes a high degradation of myocyte proteins and myocyte death by mechanisms of apoptosis, autophagy and necrosis [53,54], eventually contributing to the heart weight loss [55]. Furthermore, when evaluating the extent of heart inflammation caused by CVB3 infection, the body weight of the mice needs to be mulled together since severe loss of body weight also happened in the CVB3-infected mice. To reflect this, we also used heart / body weight ratio to evaluate the extent of the heart inflammation [56], and found that the ratio was increased in the mice treated with AAAG ODN on day −1 and decreased in the mice treated with AAAG ODN on day 4.

In addition to TLR9, TLR4 is another IRF5 regulating receptor involved in the development of CVB3-induced myocarditis [57]. Activation of TLR4-IRF5 signaling pathway mediates transcription of the IL-1β, IL-12, IL-8 [58] and RANTES (regulated upon activation normal T cells expressed and secreted) genes [59]. The increased expression of these cytokines was observed in blood or left ventricle in CVB-infected mice [60,61], accompanied with the vigorous CVB3 replication and cardiac dysfunction [62]. The data are instructive to investigate the roles of TLR4-IRF5 signaling pathway molecules in the development of CVB3-induced myocarditis. The TLR4 involvement may remind us to find whether receptor for advanced glycation end products (RAGE) could also play a role in the development of CVB3-induced myocarditis because that RAGE also induces the production of TNF-α and IL-6, and its short cytoplasmic tail is highly homologous to TLR4 cytoplasmic Toll/interleukin-1 receptor [63].

## Acknowledgements

This study was supported by National Nature Scientific Foundation of China (31670937 and 81570002).

## References

[1] N.R. Rose, Viral myocarditis, J. Curr Opin Rheumatol. 28 (2016) 383–389, https://doi.org/10.1097/BOR.0000000000000303.
[2] U. Kühl, M. Pauschinger, M. Noutsias, B. Seeberg, T. Bock, D. Lassner, W. Poller, R. Kandolf, H.P. Schultheiss, High prevalence of viral genomes and multiple viral infections in the myocardium of adults with“idiopathic”left ventricular dysfunction, J. Circulation. 111 (2005) 887–893, https://doi.org/10.1161/01.CIR.0000155616.07901.35.
[3] S. Heymans, U. Eriksson, J. Lehtonen, L.T. Cooper Jr., The quest for new approaches in myocarditis and inflammatory cardiomyopathy, J. Am. Coll. Cardiol. 68 (2016) 2348–2364, https://doi.org/10.1016/j.jacc.2016.09.937.
[4] Toshitaka Yajima, Viral myocarditis: potential defense mechanisms within the cardiomyocyte against virus infection, J. Future Microbiol. (5) (2011) 551–566, https://doi.org/10.2217/fmb.11.40.
[5] A. Riad, D. Westermann, F. Escher, P.M. Becher, K. Savvatis, O. Lettau, M.M. Heimesaat, S. Bereswill, H.D. Volk, H.P. Schultheiss, C. Tschöpe, Myeloid differentiation factor-88 contributes to TLR9-mediated modulation of acute coxsackievirus B3-induced myocarditis in vivo, J. Physiol Heart Circ Physiol. 298 (2010) 2024–2031, https://doi.org/10.1152/ajpheart.01188.2009.
[6] L. Liaudet, N. Rosenblatt-Velin, Role of innate immunity in cardiac inflammation after myocardial infarction, J. Front Biosci. 5 (2013) 86–104, https://doi.org/10.2741/S359.
[7] G.N. Barber, Innate immune DNA sensing pathways: STING, AIMII and the regulation of interferon production and inflammatory responses, J. Curr Opin Immunol. 23 (2011) 10–20, https://doi.org/10.1016/j.coi.2010.12.015.
[8] E.I. Lafferty, S.A. Wiltshire, I. Angers, S.M. Vidal, S.T. Qureshi, Unc93b1 -dependent Endosomal toll-like receptor Signaling regulates inflammation and mortality during Coxsackievirus B3 infection, J. Innate Immun. 3 (2015) 315–330, https://doi.org/10.1159/000369342.
[9] J.L. Bao, L. Lin, MiR-155 and miR-148a reduce cardiac injury by inhibiting NF-κB pathway during acute viral myocarditis, J, Eur. Rev. Med. Pharmacol. Sci. 18 (2014) 2349–2356.
[10] F. Steinhagen, A.P. McFarland, L.G. Rodriguez, P. Tewary, A. Jarret, R. Savan, D.M. Klinman, IRF-5 and NF-κB p50 co-regulate IFN-β and IL-6 expression in TLR9-stimulated human plasmacytoid dendritic cells, J. Eur J Immunol. 43 (2013) 1896–1906, https://doi.org/10.1002/eji.201242792.
[11] A. Takaoka, H. Yanai, S. Kondo, G. Duncan, H. Negishi, T. Mizutani, S. Kano, K. Honda, Y. Ohba, T.W. Mak, T. Taniguchi, Integral role of IRF-5 in the gene induction programme activated by toll-like receptors, J. Nature. 434 (2005) 243–249, https://doi.org/10.1038/nature03308.
[12] A. Paun, J.T. Reinert, Z. Jiang, C. Medin, M.Y. Balkhi, K.A. Fitzgerald, P.M. Pitha, Functional characterization of murine interferon regulatory factor 5 (IRF-5) and its role in the innate antiviral response, J. Biol. Chem. 283 (2008) 14295–14308, https://doi.org/10.1074/jbc.M800501200.
[13] T. Kanda, T. Takahashi, Interleukin-6 and cardiovascular diseases, J. Jpn Heart J. 45 (2004) 183–193, https://doi.org/10.1536/jhj.45.183.
[14] J. Shu, L. Li, L.B. Zhou, J. Qian, Z.D. Fan, L.L. Zhuang, L.L. Wang, R. Jin, H.G. Yu, G.P. Zhou, IRF5 is elevated in childhood-onset SLE and regulated by histone acetyltransferase and histone deacetylase inhibitors, J. Oncotarget. 29 (2017) 47184–47194, https://doi.org/10.18632/oncotarget.17586.
[15] L. Peng, H. Zhang, Y. Hao, F. Xu, J. Yang, R. Zhang, G. Lu, Z. Zheng, M1. Cui, C.F. Qi, C. Chen, J. Wang, Y. Hu, D. Wang, S. Pierce, L. Li, H. Xiong, Reprogramming macrophage orientation by microRNA 146b targeting transcription factor IRF5, J. EBioMedicine. 14 (2016) 83–96, https://doi.org/10.1016/j.ebiom.2016.10.041.
[16] D. Weihrauch, J.G. Krolikowski, D.W. Jones, T. Zaman, O. Bamkole, J. Struve, S. Pillai, P.S. Pagel, N.L. Lohr, K.A. Pritchard Jr., An IRF5 Decoy Peptide Reduces Myocardial Inflammation and Fibrosis and Improves Endothelial Cell Function in Tight-Skin Mice, J. PLoS One. 4 (2016) e0151999, , https://doi.org/10.1371/journal.pone.0151999.
[17] M. Fang, M. Wan, S. Guo, R. Sun, M. Yang, T. Zhao, Y. Yan, Y. Zhang, W. Huang, X. Wu, Y. Yu, L. Wang, S. Hua, An oligodeoxynucleotide capable of lessening acute lung inflammatory injury in mice infected by influenza virus, J. Biochem Biophys Res Commun. 415 (2011) 342–347, https://doi.org/10.1016/j.bbrc.2011.10.062.
[18] S. Gao, X. Li, S. Nie, L. Yang, L. Tu, B. Dong, P. Zhao, Y. Wang, Y. Yu, L. Wang, S. Hua, An AAAG-rich Oligodeoxynucleotide rescues mice from bacterial septic peritonitis by interfering interferon regulatory factor 5, J. Int J Mol Sci. 18 (2017), https://doi.org/10.3390/ijms18051034 pii: E1034.
[19] Y. Xiao, W. Lu, X. Li, P. Zhao, Y. Yao, X. Wang, Y. Wang, Lin Z1, Yu Y, Hua S, Wang L, An oligodeoxynucleotide with AAAG repeats significantly attenuates burn-induced systemic inflammatory responses via inhibiting interferon regulatory factor 5 pathway, J. Mol. Med. 23 (2017) 166–176, https://doi.org/10.2119/molmed.2016.00243.
[20] Chinese Heart Association, The diagnostic criteria of myocarditis, J. Chinese Journal of Practical Pediatrics. 15 (2000) 75.
[21] M.R. Hazebroek, K. Everaerts, S. Heymans, Diagnostic approach of myocarditis: strike the golden mean, J. Neth Heart J. 2 (2014) 80–84, https://doi.org/10.1007/s12471-013-0499-3.
[22] Y. Ren, L. Hua, X. Meng, Y. Xiao, X. Hao, S. Guo, P. Zhao, L. Wang, B. Dong, Y. Yu, L. Wang, Correlation of surface toll-like receptor 9 expression with IL-17 production in neutrophils during septic peritonitis in mice induced by E. coli, J. Mediators Inflamm. (2016) 3296307, , https://doi.org/10.1155/2016/3296307.
[23] M. Aly, S. Wiltshire, G. Chahrour, J.C. Osti, S.M. Vidal, Complex genetic control of host susceptibility to coxsackievirus B3-induced myocarditis, J. Genes Immun. 3 (2007) 193–204, https://doi.org/10.1038/sj.gene.6364374.
[24] L. J, H. Muench, A simple method of estimating fifty percent endpoints, J. Am J Hyg. 27 (1938) 493–497, https://doi.org/10.1093/oxfordjournals.aje.a118408.
[25] L. Yang, L. Sun, X. Wu, L. Wang, H. Wei, M. Wan, P. Zhang, Y. Yu, L. Wang, Therapeutic injection of C-class CpG ODN in draining lymph node area induces potent activation of immune cells and rejection of established breast cancer in mice, J. Clin. Immunol. (3) (2009) 426–437, https://doi.org/10.1016/j.clim.2009.01.011.
[26] Z. Wang, X. Wu, Y. Zhang, L. Zhou, L. Li, Y. Yu, L. Wang, Discrepant roles of CpG ODN on acute alcohol-induced liver injury in mice, J. Int Immunopharmacol. 12 (2012) 526–533, https://doi.org/10.1016/j.intimp.2012.01.007.
[27] F.C. Hankenson, N. Ruskoski, M. van Saun, G.S. Ying, J. Oh, N.W. Fraser, Weight loss and reduced body temperature determine humane endpoints in a mouse model of ocular herpesvirus infection, J. J Am Assoc Lab Anim Sci. 52 (2013) 277–285, https://doi.org/10.1186/1746-6148-9-89.
[28] S. Omura, E. Kawai, F. Sato, N.E. Martinez, G.V. Chaitanya, P.A. Rollyson, U. Cvek, M. Trutschl, J.S. Alexander, I. Tsunoda, Bioinformatics multivariate analysis determined a set of phase-specific biomarker candidates in a novel mouse model for viral myocarditis, J. Circ Cardiovasc Genet. (4) (2014) 444–454, https://doi.org/10.1161/CIRCGENETICS.114.000505.
[29] J.J. Greer, D.P. Ware, D.J. Lefer, Myocardial infarction and heart failure in the db/db diabetic mouse, J. Am J Physiol Heart Circ Physiol. (1) (2006) H146–H153, https://doi.org/10.1152/ajpheart.00583.2005.
[30] W. Zhang, K.J. Lavine, S. Epelman, S.A. Evans, C.J. Weinheimer, P.M. Barger, D.L. Mann, Necrotic myocardial cells release damage-associated molecular patterns that provoke fibroblast activation in vitro and trigger myocardial inflammation and fibrosis in vivo, J. Heart Assoc. 4 (2015) e001993, , https://doi.org/10.1161/JAHA.

115.001993.
[31] M. Bliksøen, L.H. Mariero, I.K. Ohm, F. Haugen, A. Yndestad, S. Solheim, I. Seljeflot, T. Ranheim, G.Ø. Andersen, P. Aukrust, G. Valen, L.E. Vinge, Increased circulating mitochondrial DNA after myocardial infarction, J. Cardiol. 58 (2012) 132–134, https://doi.org/10.1016/j.ijcard.2012.04.047.
[32] Y. Yu, Y. Yu, M. Liu, P. Yu, G. Liu, Y. Liu, Y. Su, H. Jiang, R. Chen, Ethyl pyruvate attenuated coxsackievirus B3-induced acute viral myocarditis by suppression of HMGB1/RAGE/NF-KB pathway, J. Springerplus. 5 (2016) 215, https://doi.org/10.1186/s40064-016-1857-6.
[33] T. Oka, S. Hikoso, O. Yamaguchi, M. Taneike, T. Takeda, T. Tamai, J. Oyabu, T. Murakawa, H. Nakayama, K. Nishida, S. Akira, A. Yamamoto, I. Komuro, K. Otsu, Mitochondrial DNA that escapes from autophagy causes inflammation and heart failure, J. Nature. 7397 (2012) 251–255, https://doi.org/10.1038/nature10992.
[34] Maarten F. Corsten, Blanche Schroen, Stephane Heymans, Inflammation in viral myocarditis: friend or foe? J. Trends Mol Med. (7) (2012) 426–437, https://doi.org/10.1016/j.molmed.2012.05.005.
[35] Yan Feng, Wei Chao, Toll-like receptors and myocardial inflammation, J. Inflamm. (2011) 170352, https://doi.org/10.4061/2011/170352.
[36] J. Tian, A.M. Avalos, S.Y. Mao, B. Chen, K. Senthil, H. Wu, P. Parroche, S. Drabic, D. Golenbock, C. Sirois, J. Hua, L.L. An, L. Audoly, G. La Rosa, A. Bierhaus, P. Naworth, A. Marshak-Rothstein, M.K. Crow, K.A. Fitzgerald, E. Latz, P.A. Kiener, A.J. Coyle, Toll-like receptor 9-dependent activation by DNA-containing immune complexes is mediated by HMGB1 and RAGE, J. Nat Immunol. 5 (2007) 487–496, https://doi.org/10.1038/ni1457.
[37] E.R. Kandimalla, F.G. Zhu, L. Bhagat, D. Yu, S. Agrawal, Toll-like receptor 9: modulation of recognition and cytokine induction by novel synthetic CpG DNAs, J. Biochem Soc Trans. 31 (2003) 654–658, https://doi.org/10.1042/bst0310654.
[38] A.L. Blasius, B. Beutler, Intracellular toll-like receptors, J. Immunity. 32 (2010) 305–315, https://doi.org/10.1016/j.immuni.2010.03.012.
[39] W. Zhu, J. Yu, S. Qiu, H. Liu, Y. Wang, X. Xu, L. Shao, L. Zhu, Y. Jiao, F. Liu, X. Zhu, MiR-let-7a regulates anti-citrullinated protein antibody-induced macrophage activation and correlates with the development of experimental rheumatoid arthritis, J. Int Immunopharmacol. 51 (2017) 40–46, https://doi.org/10.1016/j.intimp.2017.08.001.
[40] W. Zhu, Z. Jin, J. Yu, J. Liang, Q. Yang, F. Li, X. Shi, X. Zhu, X. Zhang, Baicalin ameliorates experimental inflammatory bowel disease through polarization of macrophages to an M2 phenotype, J. Int Immunopharmacol. 35 (2016) 119–126, https://doi.org/10.1016/j.intimp.2016.03.030.
[41] N. Tanaka, T. Kawakami, T. Taniguchi, Recognition DNA sequences of interferon regulatory factor 1 (IRF -1) and IRF -2, regulators of cell growth and the interferon system. 2, regulators of cell growth and the interferon system, J. Mol. Cell Biol. 13 (1993) 4531–4538, https://doi.org/10.1128/mcb.13.8.4531.
[42] A. Miyawaki, M. Obana, Y. Mitsuhara, A. Orimoto, Y. Nakayasu, T. Yamashita, S.I. Fukada, M. Maeda, H. Nakayama, Y. Fujio, Adult murine cardiomyocytes exhibit regenerative activity with cell cycle reentry through STAT3 in the healing process of myocarditis, J. Sci Rep. 7 (2017) 1407, https://doi.org/10.1038/s41598-017-01426-8.
[43] J.H. Du, N. Xu, Y. Song, M. Xu, Z.Z. Lu, C. Han, Y.Y. Zhang, AICAR stimulates IL-6 production via p38 MAPK in cardiac fibroblasts in adult mice: a possible role for AMPK, J. Biochem Biophys Res Commun. 337 (2005) 1139–1144, https://doi.org/10.1016/j.bbrc.2005.09.174.
[44] H.P. Lauritzen, J. Brandauer, P. Schjerling, H.J. Koh, J.T. Treebak, M.F. Hirshman, H. Galbo, L.J. Goodyear, Contraction and AICAR stimulate IL-6 vesicle depletion from skeletal muscle fibers in vivo, J. Diabetes. 9 (2013) 3081–3092, https://doi.org/10.2337/db12-1261.
[45] Z.H. Lin, Y.C. Li, S.J. Wu, C. Zheng, Y.Z. Lin, H. Lian, W.Q. Lin, J.F. Lin, Eliciting α7-nAChR exerts cardioprotective effects on ischemic cardiomyopathy via activation of AMPK signalling, J. J Cell Mol Med. (2019), https://doi.org/10.1111/jcmm.14363.
[46] S.C. Bairwa, N. Parajuli, J.R. Dyck, The role of AMPK in cardiomyocyte health and survival, J. Biochim Biophys Acta. 1862 (2016) 2199–2210, https://doi.org/10.1016/j.bbadis.
[47] C. Weigert, M. Düfer, P. Simon, E. Debre, H. Runge, K. Brodbeck, H.U. Häring, E.D. Schleicher, Upregulation of IL-6 mRNA by IL-6 in skeletal muscle cells: role of IL-6 mRNA stabilization and $Ca^{2+}$-dependent mechanisms, J. Am J Physiol Cell Physiol. 393 (2007) C1139–C1147, https://doi.org/10.1152/ajpcell.00142.2007.
[48] F. Chen, D. Chen, Y. Zhang, L. Jin, H. Zhang, M. Wan, T. Pan, X. Wang, Y. Su, Y. Xu, J. Ye, Interleukin-6 deficiency attenuates angiotensin II-induced cardiac pathogenesis with increased myocyte hypertrophy, J. Biochem Biophys Res Commun. 494 (2017) 534–541, https://doi.org/10.1016/j.bbrc.
[49] A.E. Mayfield, P. Kanda, A. Nantsios, S. Parent, S. Mount, S. Dixit, B. Ye, R. Seymour, D.J. Stewart, D.R. Davis, Interleukin-6 mediates post-infarct repair by cardiac explant-derived stem cells, J. Theranostics. 7 (2017) 4850–4861, https://doi.org/10.7150/thno.19435.
[50] D. Aderka, J.M. Le, J. Vilcek, IL-6 inhibits lipopolysaccharide-induced tumor necrosis factor production in cultured human monocytes, U937 cells, and in mice, J. J Immunol. 11 (1989) 3517–3523.
[51] R. Schindler, J. Mancilla, S. Endres, R. Ghorbani, S.C. Clark, C.A. Dinarello, Correlations and interactions in the production of interleukin-6 (IL-6), IL-1, and tumor necrosis factor (TNF) in human blood mononuclear cells: IL-6 suppresses IL-1 and TNF, J. Blood. 1 (1990) 40–47, https://doi.org/10.1002/ajh.2830330118.
[52] P. Price, D.M. Murdoch, U. Agarwal, S.R. Lewin, J.H. Elliott, M.A. French, Immune restoration diseases reflect diverse immunopathological mechanisms, J. Clin Microbiol Rev. 22 (2009) 651–663, https://doi.org/10.1128/CMR.00015-09.
[53] S. Pérez-Baos, I. Prieto-Potin, J.A. Román-Blas, O. Sánchez-Pernaute, R. Largo, G. Herrero-Beaumont, Mediators and patterns of muscle loss in chronic systemic inflammation, J. Front Physiol. 9 (2018) 409, https://doi.org/10.3389/fphys.2018.00409.
[54] P.R. Rao, R.K. Viswanath, Cardioprotective activity of silymarin in ischemia-reperfusion-induced myocardial infarction in albino rats, J. Exp. Clin. Cardiol. 4 (2007) 179–187, https://doi.org/10.1007/s00395-012-0288-y.
[55] T.A. Zimmers, Y. Jiang, M. Wang, T.W. Liang, J.E. Rupert, E.D. Au, F.E. Marino, M.E. Couch, L.G. Koniaris, Exogenous GDF11 induces cardiac and skeletal muscle dysfunction and wasting, J. Basic Res Cardiol. 112 (2017) 4, https://doi.org/10.1007/s00395-017-0639-9.
[56] S. Omura, E. Kawai, F. Sato, N.E. Martinez, G.V. Chaitanya, P.A. Rollyson, U. Cvek, M. Trutschl, J.S. Alexander, I. Tsunoda, Bioinformatics multivariate analysis determined a set of phase-specific biomarker candidates in a novel mouse model for viral myocarditis, J. Circ Cardiovasc Genet. 7 (2014) 444–454, https://doi.org/10.1161/circgenetics.114.000505.
[57] M. Satoh, M. Nakamura, T. Akatsu, J. Iwasaka, Y. Shimoda, I. Segawa, K. Hiramori, Expression of toll-like receptor 4 is associated with enteroviral replication in human myocarditis, J. Clin Sci (Lond). (6) (2003) 577–584, https://doi.org/10.1042/cs20020263.
[58] S.S. Reddy, P. Chauhan, P. Maurya, D. Saini, P.P. Yadav, M.K. Barthwal, Coagulin-L ameliorates TLR4 induced oxidative damage and immune response by regulating mitochondria and NOX-derived ROS, J. Toxicol Appl Pharmacol. 309 (2016) 87–100, https://doi.org/10.1016/j.taap.2016.08.022.
[59] M. Rodríguez-Valentín, S. López, M. Rivera, E. Ríos-Olivares, L. Cubano, N.M. Boukli, Naturally derived anti-HIV polysaccharide peptide (PSP) triggers a toll-like receptor 4-dependent antiviral immune response, J. J Immunol Res. 2018 (2018) 1–14, https://doi.org/10.1155/2018/8741698.
[60] T. Han, K. Zhao, C. Wu, H. Lu, D. Song, W. He, F. Gao, Viral kinetics are associated with changes in cytokines and chemokines in serum and target organs of SSM-CVB3-infected macaques, J. Exp Mol Pathol. (1) (2013) 174–181, https://doi.org/10.1016/j.yexmp.2012.06.006.
[61] M. Lundgren, P.O. Darnerud, J. Blomberg, G. Friman, N.G. Ilbäck, Sequential changes in serum cytokines reflect viral RNA kinetics in target organs of a coxsackievirus B infection in mice, J. Clin. Immunol. (5) (2009) 611–619, https://doi.org/10.1007/s10875-009-9294-8.
[62] K. Miteva, K. Pappritz, M. El-Shafeey, F. Dong, J. Ringe, C. Tschöpe, S. Van Linthout, Stem Cells Translational Medicine, J. 6 (2017) 1249–1261, https://doi.org/10.1007/s10875-009-9294-8.
[63] M. Sakaguchi, R. Kinoshita, E.W. Putranto, I.M.W. Ruma, I.W. Sumardika, C. Youyi, N. Tomonobu, K.I. Yamamoto, H. Murata, Signal diversity of receptor for advanced Glycation end products, J. Acta Med Okayama. 6 (2017) 459–465, https://doi.org/10.18926/AMO/55582.
[64] Martin Dolgin, New York, Heart Association. Criteria Committee Nomenclature and Criteria for Diagnosis of Diseases of the Heart and Great Vessels, 9th ed. / editor, Martin Dolgin Little, Brown, Boston (1994), pp. 253–256.